Translational, vibrational, rotational enhancements and alignments of reactions H + ClF ($v = 0$–5, $j = 0, 3, 6, 9$) →HCl + F and HF + Cl, at $E_{rel} = 0.5$–20 kcal/mol*

Victor Wei-Keh Chao(Wu) (赵(吴)为克)[a)b)c)†]

[a)] *Department of Chemical and Materials Engineering, National Kaohsiung University of Applied Sciences, 80782 Kaohsiung City, Taiwan, China*
[b)] *Group 1101, State Key Laboratory of Molecular Reaction Dynamics, Dalian Institute of Chemical Physics, Chinese Academy of Sciences, Dalian 116023, China*
[c)] *Victor Basic Research Laboratory e. V. Gadderbaumer-Str. 22, D-33602 Bielefeld, Germany*

(Received 4 February 2013; revised manuscript received 31 March 2013)

Quasi-classical trajectory calculations of the title reactions H + ClF ($v = 0$–5, $j = 0, 3, 6, 9$) → HCl + F and H + ClF ($v = 0$–5, $j = 0, 3, 6, 9$) → HF + Cl at $E_{rel} = 0.5$ kcal/mol–20 kcal/mol on ground potential energy surface DHTSN of 1 ^{2}A′ [M. P. Deskevich, M. Y. Hayes, K. Takahashi, R. T. Skodje and D. J. Nesbitt, *J. Chem. Phys.* **124**, 224303 (2006)] are performed. Potential energy surfaces derived from DHTSN for the title reactions are obtained, and compared with that of DHTSN for the reaction F + HCl → HF + Cl. Both potential energy surfaces have an early barrier pattern. Integral cross sections and alignments of product molecules HCl and HF dependent on the internal energy states v and j of reactant molecule ClF are obtained and compared. Translational, vibrational, and rotational energy specific translational enhancements of the reactant molecule ClF of the title reactions are found. Reaction mechanisms of the title reactions according to the respective potential energy contours are further found and explained. Reasons of simultaneous translational and vibrational enhancements are clarified.

Keywords: quasi-classical trajectory calculation, integral cross section, alignment, TRV enhancement

PACS: 31.15.xv, 31.50.Bc, 34.20.−b, 82.20.Bc **DOI:** 10.1088/1674-1056/22/10/103101

1. Introduction

An investigation to describe and solve the problem of a three-atomic reaction system with H_3 originated in London in 1929.[1,2] It was a landmark in the history of chemistry, comparable to the landmark in the history of physics due to the advent of the Heitler–London equation[3] for H_2. Eyring and Polanyi[4] obtained in 1931 the first potential energy surface (PES) for H_3 after the Heitler–London equation. Since modification with the Sato parameter by Sato,[5–7] the classical PES known as LEPS has appeared as standard and applicable until now. The fundamental analyses of chemical reaction dynamics with a three atomic system $A + BC$ for the construction of a general PES (LEPS) with three pairs of diatomic potential energy curves of *AB*, *BC*, and *CA* were carried out firstly by Sato[5–7] after London, Eyring and Polanyi,[5–15] where *A* denotes an atom and *BC* represents a diatomic molecule. The three-atomic chemical reaction dynamics with system $A + BC$ were analyzed,[16–24] and classified into all possible combinations of heavy and light atoms.[13,17–19] Their results have been cited by many publications of experimental, simulation, or calculation work until now.

Potential energy surface is a virtual surface or constructed platform, e.g. LEPS, on which a process of a chemical reaction is simulated. A three-atomic model or system with atoms *A*, *B*, and *C* is typical and standard for investigating the reaction dynamics — reactants *A* and *BC* interact and collide together with or without nascent *ABC* appearing in a short time separate into new products *AB* and *C* in a short time. There are considered not only translational energies of *A*, *BC*, *AB*, and *C*, but also internal (vibrational and rotational) energies of *BC* and *AB*. Since the pioneering work by Wall, Hiller, and Mazur in 1958,[8,9] the Monte Carlo method has been used to simulate a chemical reaction procedure, path or trajectory on a respective LEPS surface.[9,14]

Based on Newtonian mechanics and quantum energy states of vibration and rotation of the reactant and product molecules, quasiclassical trajectory (QCT) is one of the methods to simulate chemical reaction dynamics,[25–32] where the alignment[25,26] and rotational polarization of the product molecule have also been integrated.[27–32]

Many kinds of systems have been investigated in the last long years. Of them, HClF three-atomic system has received the most attention in the last 10 years, regarding to the problems of combustion, energy resource, and pollution. The necessary way to solve the problem thoroughly is to understand the basic reaction mechanism. There have been several investigations of this system, with reactions F + HCl → HF + Cl,[21,33–43] H + ClF → HF + Cl,[23,24,44–52] and H + ClF → HCl + F.[25,26,44–52] Among those reports, the work in nine experimental reports[21,23,40–45,48] were done more than 30 years

*Project supported by the State Key Laboratory of Molecular Reaction Dynamics, Dalian Institute of Chemical Physics, Chinese Academy of Sciences (Grant No. 2012-1101-1) and Victor Basic Research Laboratory e. V. in Bielefeld, Germany.

†Corresponding author. E-mail: victorbres3tw@yahoo.com.tw

© 2013 Chinese Physical Society and IOP Publishing Ltd

ago. Since these works, there have been rather few investigations on this HClF system. There was only the theoretical exploration of the variational transition state theory by calculating the rate constants of the $F + HCl \rightarrow Cl + HF$, $H + ClF \rightarrow HF + Cl$, and $H + ClF \rightarrow HCl + F$ reactions[33,34] in 1999. Recently, there were several dynamic investigations of either $H + ClF \rightarrow HCl + F$ or $H + ClF \rightarrow HF + Cl$ reactions by using the QCT methods.[49,50] However, its reverse reaction has attracted much attention and has been studied in detail both experimentally and theoretically[21,22,29,30,53–56] to unravel several issues such as reactive resonance,[56,57] nonadiabatic dynamics,[57–60] hydrogen halide chemical lasers,[61] etc. Up to date, potential energy surfaces (PESs) used for calculating quantum scattering or quasiclassical trajectory for the title reactions include PES of Sayós *et al.*[33,34] for the ground $1\ ^2A'$ state at the PUMP2/6-311G(3d2f, 3p2d) calculation level, empirical LEPS PES of Kornweitz and Persky[42] for the ground $1\ ^2A'$ state, diabatic potential matrix of Fishchuk *et al.*[43] for the lowest three states for nonadiabatic dynamics, and the ground state DHTSN PES.[36] All of these PESs have been employed previously in dynamical explorations of the $F + HCl$ system, and the DHTSN PES[36] is most used in recent scattering probes of the reactive system due to the fact that it has been the most accurate PES thus far with a high MRCI + Q/aug-cc-pVnZ ($n = 2,3,4$) calculation level.

The incomplete investigation of the title reactions thus stimulates the series of our calculations.[49,50] Product HF angular momentum polarizations in the reaction $H + ClF$ ($v = 0$–5, $j = 0,3,6,9$) $\rightarrow HF + Cl$, including the integral cross sections and alignments of HF and HCl dependent on the relative translational energies E_{rel} of both reactants and vibrational energies of reactant molecule ClF, within the same range of E_{rel} by using QCT method have been reported in the last paper.[49,50] The motivation to choose this mass combination $L + H_1H_2$, in which $H_1/H_2 \approx 1/2$ after the investigation series of $O + H_2$ (model $H + L_1L_2$, with $L_1/L_2 = 1$)[62] and $O + HD$ (model $H + L_1L_2$ with $L_1/L_2 = 1/2$)[63,64] where H_1, H_2, L_1, and L_2 represent heavy and light atoms with numerical subscript indexes 1 and 2 to distinguish the atoms, is to investigate how far the mass combination either $L + H_1/H_2$ or $H + L_1/L_2$ of the reactants influences the stereo chemical reaction dynamics as well as transformational reaction dynamics. The mass combination $H + L_1L_2$ may be applicable for the docking mechanism, which sounds irrelevant.[64] There are both translational and vibrational enhancements with potential energy barriers located in the entrance channels for the title reactions found.[49,50] The product molecule HF is manifestly scattered forwards;[49,50] HCl is scattered backwards.[65] In order to clarify the translational and vibrational enhancements on the PESs with similar early barriers for the title reactions, detailed investigations and comparisons are necessary. In this paper, results of translational, vibrational, rotational enhancements of ClF and alignments of HF and HCl were summarized. The product molecular rotational angular momentum polarizations of HCl compared with those of HF[49,50] were presented in the coming paper,[65] because of the immense data quantity.

The program "Symplectic" of the QCT method, which is the same as that used for previous work,[49,50,62–64,66–76] has been applied to the title reactions. The DHTSN PES is inserted into this program as one of the input data sets. The procedure of this work can be classified as follows:

(i) DHTSN PES with coordinates (r_{HF}, r_{HCl}, V) is plotted in order to see whether the data has a significant equivalence with the original (Fig. 8 in Ref. [36]).

(ii) Contour maps (r_{HCl}, r_{ClF}, V) and (r_{HF}, r_{ClF}, V) with the respective incoming and outgoing channels, known as entrance and exit valleys, respectively, of the title reactions from DHTSN PES are obtained. Two maps with the transition state geometries[77,78] of both [H–Cl–F] and [H–F–Cl], at two bent angles 90° and 120° of the transition complex for two title reactions are obtained and plotted.

(iii) Integral cross sections of HCl and HF dependent on the relative translational energies E_{rel} of the reactants and also dependent on the set of vibrational and rotational states (v, j) of the reactant molecule ClF are obtained.

(iv) Alignments p_2 of the product molecules HCl and HF dependent on the relative translational energy E_{rel} and vibrational state of the reactant molecule ClF are also obtained.

The detailed calculation and evaluation procedures are described. Both potential energy surfaces obtained from DHTSN PES belong to the early barrier pattern. The influences of the PESs as well as potential energy contours, translational, vibrational, and rotational enhancements of the reactant molecule ClF for the title reactions at $E_{rel} = 0.5$ kcal/mol–20 kcal/mol are obtained, compared, and discussed. Reaction mechanisms of the title reactions according to the respective potential energy contours are obtained. Reasons for the simultaneous translational and vibrational enhancements are conveyed.

2. Method and computation

Han *et al.*[25,79] calculated the reaction product rotational polarization using the QCT method in 1993, which makes it possible to compare the theoretical rotational polarizations[25] with experimental values[79,80] directly. The theoretical formalism as well as procedure of the computation, the quasiclassical trajectory polarization-dependent differential cross section (QCT-PDDCS) code "Symplectic" used in this work has been developed by Han and Sun,[31] and validated by Xie *et al.*[59] and Chu *et al.*[60] for studying chemical reaction dynamics. The stereodynamic calculation method and code are the same as those used in Refs. [49]–[52], [62]–[76], [79], and [80]. DHTSN PES[36] $1\ ^2A'$ being inserted into this trajectory program, we present the calculated integral cross sections and alignments of the product molecules HCl and HF

dependent on the relative collision energy E_{rel} in a range of 0.5 kcal/mol–20 kcal/mol of the reactants H and molecule ClF, with the vibrational and rotational energies ($v = 0$–5, $j = 0$, 3, 6, and 9) of the reactant molecule ClF of the title reactions with QCT-PDDCS code.

The QCT-PDDCS program is a trajectory simulation or calculation program, and provides very detailed informations[49,50] about the reaction procedure (Table 1) on the PES chosen, and production of the product molecules of either HCl or HF, dependent on the relative collision energy E_{rel}, polar θ_r, and azimuthal φ_r angle shown in Fig. 1. The necessary input parameters are the start distance between the reactants, maximum impact parameter, number of trajectories intended, mass values of A, B, and C, collision energy (relative collision energy E_{rel}), potential energy curve depths, equilibrium distances, and morse parameters of the three pairs of the diatomic molecules (AB, BC, and AC), and Monte-Carlo number production function for the impact parameter, with which the approach of the reactants as well as how the reaction starts can be initiated. Information which can be obtained is as follows:

a) integral cross sections of the products or product molecules, which are dependent on the collision energy E_{rel},

b) alignments of the product molecules, which are dependent on the collision energy,

c) polar angular distribution $p(\theta_r)$ of the product molecules,

d) azimuthal angular distribution $p(\varphi_r)$ of the product molecules,

e) dihedral angular distribution $p(\theta_r, \varphi_r)$ of the product molecules, and

f) the four polarization-dependent differential cross sections (PDDCSs), which are dependent on the scattering angle θ_t of the product molecules, either HCl or HF of the title reactions at a given collision energy E_{rel}.

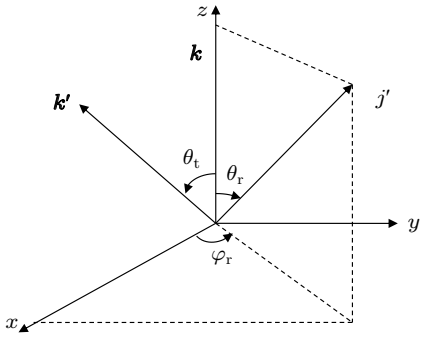


Fig. 1. Schematical illustration of the vector correlations in the center of mass (CM) frame.

Table 1. Distributions of the values of impact parameter b_{max}, number of reactive trajectories n, integral cross section σ, and alignment p_2 ($= \langle \boldsymbol{j}' \cdot \boldsymbol{k} \rangle$) for the product molecules HCl and HF, dependent on the relative scattering energies 0.5 kcal/mol–20 kcal/mol, with 10^4 batches, for reaction $H + ClF(v = 0, j = 0) \rightarrow HCl(v', j') + F$ and $HF(v', j') + Cl$.

Product	HCl				HF			
E_{rel}/kcal·mol^{-1}	b_{max}/Å	n_{HCl}	σ_{HCl}/Å^2	p_2	b_{max}/Å	n_{HF}	σ_{HF}/Å^2	p_2
0.5	2.525	48	0.09614	−0.2882	1.5	7	0.00495	−0.4216
1.0	2.6875	102	0.2314	−0.2521	1.9	39	0.0442	−0.385
2.0	2.75	184	0.43715	−0.2792	2.0	86	0.1081	−0.3008
2.5	2.825	199	0.4989	−0.2007	2.6	73	0.1550	−0.3081
5.0	2.855	303	0.7759	−0.2683	2.855	127	0.3252	−0.2207
7.5	2.9	404	1.0674	−0.2900	2.95	148	0.4046	−0.1884
10.0	2.375	695	1.2316	−0.35475	2.308	221	0.3698	−0.1383
12.5	2.231	831	1.2994	−0.3512	2.2325	271	0.4243	−0.0896
15.0	2.25	828	1.3169	−0.3464	2.4	271	0.4904	−0.1156
17.5	2.2188	915	1.4152	−0.3046	2.24	398	0.6274	−0.0151
20.0	2.21	912	1.3994	−0.2906	2.24	460	0.7251	−0.01755

The four PDDCSs mentioned in item f) above are $PDDCS_{00}$, $PDDCS_{20}$, $PDDCS_{22+}$, and $PDDCS_{21-}$. Their significances are explained in detail elsewhere.[49,50,64] First of all, results which are reported in this paper, are limited only to i) reproduced DHTSN PES, ii) detailed descriptions of the PESs of the title reactions, iii) integral cross sections, and iv) alignments p_2 of product molecules HCl and HF dependent on E_{rel} of the reactants and the internal energy states (v, j) of the reactant molecules ClF. They are described in the introduction. p_2 given in this paper describes a mean value of the alignment of the product molecule and is dependent on the relative translational energy E_{rel} of the reactants. Distribution $PDDCS_{20}$ is another kind of description for alignment of the product molecules and is dependent on the scattering angle θ_t of the product molecule. Both kinds of presentations contribute well together to describing the alignment of the scattered product molecules. Because of the large number of results, they will be shown separately. $PDDCS_{20}$ will be given in the coming paper.[65]

Computational details are as follows: trajectories of 10^4 are running on the ground DHTSN PES[36] with the initial separation distance set to be 10 Å between the H atom and the center of mass of the ClF molecule. During the integration the time step is set to be 0.1 fs which is sufficient for obtaining

the converged results. The investigated collision energy values are 0.5, 1, 2, 2.5, 5, 7.5, 10, 12.5, 15, 17.5, and 20 kcal/mol, basically with the ClF reactant molecule initially in its ground rovibrational states of $v = 0$ and $j = 0$. The impact parameter b is one of the important input parameters. The trajectory calculation with one round of 10^4 trajectories are repeated until one of many tried impact parameters with a precision of 3 digits reaches a maximal value $b_{\max}$ after digital point has been obtained, where there no longer exists a reactive trajectory, if the further tried trajectory calculation is performed with a slightly larger value of b. The respective integral cross section, alignment, PDDCSs, and relevant others can be further obtained from this $b_{\max}$.

10^4 trajectories with the necessary input parameters mentioned were taken for one translational energy combined with one set of internal energy states of v and j of the reactant molecule ClF. The maximum start number 99999 (five numbers of 9) has been chosen for the random sampling function of the Monte-Carlo method, which produces an impact parameter b for the start of every trajectory or reaction. This maximum start sampling number has been chosen in order to achieve the highest accuracy of the results. Results obtained with 10% smaller start sampling number are approximately 0.5%–3% lower than those obtained with the maximum start sampling number. This discrepancy can be reduced down to lower than 1%, if the number of the trajectories taken is more than 5×10^4.

The simulation can run as state-to-state, i.e. with a certain combination of vibrational and rotational states (v, j) of the reactant molecule ClF used as the input, and vibrational and rotational states (v', j') of the product molecule, either HCl or HF used as the output. In this work, only results iii) Integral cross sections, and iv) Alignments of HCl and HF mentioned above, with ClF ($v = 0$, $j = 0$) at $E_{\rm rel} = 0.5$ kcal/mol–20 kcal/mol, ClF ($v = 0$, $j = 0, 3, 6, 9$) at $E_{\rm rel} = 0.5$ kcal/mol–20 kcal/mol, and ClF ($v = 0$–5, $j = 0$) at $E_{\rm rel} = 5$, 10, 15 kcal/mol, on the respective PESs of the title reactions mentioned in item ii) above are shown, compared, and discussed.

DHTSN PES[36] has been reproduced for system ClHF of the reaction $\mathrm{F} + \mathrm{HCl} \rightarrow \mathrm{HF} + \mathrm{Cl}$, corresponding to $A + BC \rightarrow AB + C$. A set of potential energies $V(r_1, r_2, r_3)$ of r_1(HF), r_2(HCl), and r_3(ClF), as $r_1(AB)$, $r_2(BC)$, and $r_3(AC)$, respectively, are received in the original package.[36] There are 418 points of $V(r_1, r_2, r_3)$ in the original DHTSN PES. They are distributed in 3 dimensions approximately $12 \times 12 \times 12\ a_0^3$ or $6 \times 6 \times 6$ Å^3, where a_0 is Bohr radius and 1 a_0 is equal to 0.52918 Å. The intermediate[77,78] of the reaction as well as system ClHF contains three atoms Cl, H, and F. The bent angle of ClHF mentioned in Ref. [36] is the angle between r_1(HF) and r_2(HCl). The information indicates that this potential energy surface may also be applicable for our title reactions, because there are the same three atoms involved in the title reactions, and three values of distance r of the interaction nuclear pairs as well as transformation intermediate are well within the ranges of the three dimensions given in DHTSN PES after the previously drawn PESs of the title reactions have been described below.

First of all, DHTSN PES is given as a reference. To show that our calculations have a correct start, i.e. on a correct PES shown in Fig. 2. The title reaction $\mathrm{H} + \mathrm{ClF} \rightarrow \mathrm{HCl} + \mathrm{F}$ can be related to $A + BC \rightarrow AB + C$. The potential energy contours shown in Figs. 3(a) and 3(b) with the intermediate at bent angles of 90° and 120° , respectively, are obtained according to the values of r_2, r_3, and $V(r_1, r_2, r_3)$ from the data of the PES of DHTSN. The values of r_2 and r_3, and $V(r_1, r_2, r_3)$ for the contour map are treated as x, y, and z values, respectively. It has an entrance valley, where H and Cl atoms approach to each other, and an exit valley, where Cl and F atoms of the reactant molecule ClF are separated after reaction. There is an early barrier, where the transformation from reactants into products occurs, on the right side of the diagonal. The intermediate at the barrier can be written as [H–Cl–F] with the possible bent angle between r_2(HCl) and r_3(ClF). The value of r_1(HF) can be obtained trigonometrically.

Another title reaction $\mathrm{H} + \mathrm{ClF} \rightarrow \mathrm{HF} + \mathrm{Cl}$ can correspond to $A + BC \rightarrow AC + B$. The potential energy contours given in Figs. 4(a) and 4(b) with intermediate at angles of 90° and 120°, respectively, are plotted with r_1, r_3, and $V(r_1, r_2, r_3)$. Values of r_1, r_3, and $V(r_1, r_2, r_3)$ for the contour map are treated as x, y, and z values, respectively. The potential energy contour is different, and has its own entrance valley, where H and F atoms come close together, and exit valley, where Cl and F atoms of ClF go apart. There is also an early barrier. The intermediate [H–F–Cl] has the possible bent angle between r_1(HF) and r_3(ClF) and r_2(HCl) can be obtained trigonometrically as well.

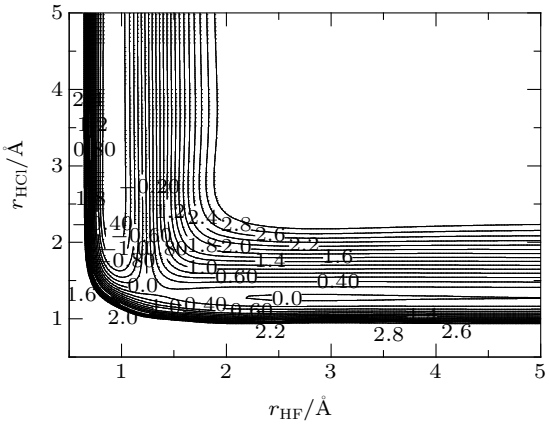


Fig. 2. Potential energy surface $V(r_{\rm HF}, r_{\rm HCl}, r_{\rm ClF})$ of DHTSN[36] for reaction $\mathrm{F} + \mathrm{HCl}\,(v, j) \rightarrow \mathrm{HF}\,(v', j') + \mathrm{Cl}$. The $r_{\rm HF}$ and $r_{\rm HCl}$ represent directions of entrance and exit valleys, respectively. The transition state geometry is [F–H–Cl] and at angle 123.5° . There is a barrier with height 3.0 kcal/mol at $(r_{\rm HF}, r_{\rm HCl}) = (1.45, 1.3)$ Å, a well with depth −1 kcal/mol at (3.0, 1.25) Å in the entrance valley; another well with depth −20 kcal/mol at $(r_{\rm HF}, r_{\rm HCl}) = (1.25, \geq 3)$ Å in the exit valley. Plot level: min = −1, max = 3, interval = 0.2 in kcal/mol, obtained with Origin 8.0.

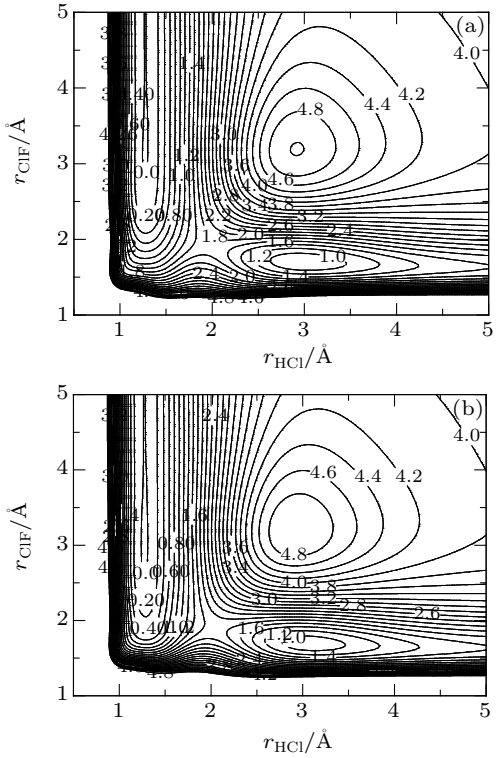


Fig. 3. Potential energy surface $V(r_{\mathrm{HCl}}, r_{\mathrm{ClF}}, r_{\mathrm{HF}})$ of DHTSN[36] for $\mathrm{H+ClF}(v,j) \rightarrow \mathrm{HCl}(v',j')+\mathrm{F}$. The r_{HCl} and r_{ClF} represent directions of entrance and exit valleys, respectively. The transition state geometry is [H–Cl–F] and at angle 90° (a). There are a barrier with height 2.1 kcal/mol at (2.0, 1.8) Å, a well with depth 0.8 kcal/mol at (3.05, 1.7) Å in entrance valley, another barrier with height 5.0 kcal/mol at (2.95, 3.1) Å on the plateau; another well with depth −50 kcal/mol at (1.3, ≥ 3.3) Å in exit valley (b) at angle 120°. There are a barrier with height 2.2 kcal/mol at (2.05, 1.75) Å, a well with depth −0.5 kcal/mol at (3.2, 1.7) Å in entrance valley, another barrier with height 5.0 kcal/mol at (3.0, 3.2) Å on the plateau; another well with depth −50 kcal/mol at (1.3, ≥ 3.5) Å in the exit valley. Plot level: min = −1, max = 5, interval = 0.2 in kcal/mol, obtained with Origin 8.0 for both angles.

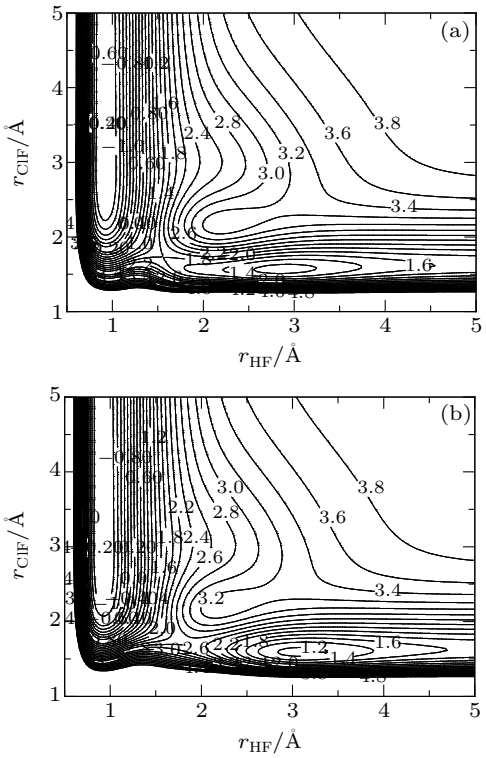


Fig. 4. Potential energy surface $V(r_{\mathrm{HF}}, r_{\mathrm{ClF}}, r_{\mathrm{HCl}})$ of DHTSN[36] for reaction $\mathrm{H+ClF}$ $(v,\ j)\rightarrow\mathrm{HF}$ $(v',j')+\mathrm{Cl}$. The r_{HF} and r_{ClF} represent directions of entrance and exit valleys, respectively. The transition state geometry is [H–F–Cl] and at angle 90° (a). There is a barrier with height 2.5 kcal/mol at (1.55, 1.65) Å, a well with depth 1.2 kcal/mol at (2.8, 1.0) Å in the entrance valley; another well with depth −20 kcal/mol at (0.85, ≥ 3.0) Å in the exit valley (b) at angle 120°. Plot level: min = −1, max = 5, intervel = 0.2 in kcal/mol with Origin 8.0. There is a barrier with height 2.6 kcal/mol at (1.8, 1.7) Å, a well with depth 1.0 kcal/mol at (3.1, 1.0) Å in the entrance valley; another well with depth −20 kcal/mol at (0.8, ≥ 2.5) Å in the exit valley. Plot level: min = −1, max = 4, intervel = 0.2 in kcal/mol with Origin 8.0.

3. Results and discussion

The reaction dynamic behaviours of $\mathrm{H+ClF \rightarrow HCl+F}$ and $\mathrm{H+ClF \rightarrow HF+Cl}$, with the reactant molecule prepared as (I) ClF ($v=0$, $j=0$) and collision energies $E_{\mathrm{rel}} = 0.5$, 1, 2, 2.5, 5, 7.5, 10, 12.5, 15, 17.5, and 20 kcal/mol; (II) ClF ($v=0$–5, $j=0$) and $E_{\mathrm{rel}} = 5$, 10, and 15 kcal/mol; (III) ClF ($v=0$, $j=0$, 3, 6, 9) and collision energies $E_{\mathrm{rel}} = 0.5$, 1, 2, 5, 10, 15, and 20 kcal/mol, have been investigated on the PESs from DHTSN[36] PES with the method of quasi-classical trajectory (QCT) calculation.

Firstly, it is tested whether the applied PES DHTSN appears for the reaction $\mathrm{F+HCl \rightarrow HF+Cl}$, the same (Fig. 2 and Table 2) as those in Fig. 8 of Ref. [36]. It is constructed with the optimized bent angle = 123.5° of the intermediate Cl–H–F.[36] It possesses a barrier with height ≥ 3.0 kcal/mol at position $(r_{\mathrm{HF}},\ r_{\mathrm{HCl}}) = (1.45, 1.30)$ Å, height of the entrance valley = −0.5 kcal/mol at (3.0, 1.25) Å; that of the exit valley = −20 kcal/mol at (1.25, ≥ 3.0) Å. The plot levels are min = −1, max = 3, and interval of the contours = 0.2, in kcal/mol, which are obtained with Origin 8.0. The respective resolutions of the contours are 0.05 Å and 0.2 kcal/mol for the coordinate and energy interval. However, the resolution must be increased to 0.01 kcal/mol so that the height of the barrier and depths of the entrance and exit valleys can occur. The ideal path of the reaction can be assumed to be along the entrance valley–barrier–exit valley route, and have the height variations 3.5 kcal/mol∼4.0 kcal/mol and 23 kcal/mol for the approach from the entrance valley to barrier, and separation from the barrier into the exit valley, respectively, within a range of 5×5 Å^2. The reaction enthalpy along this path is around -22 kcal/mol ~ -25 kcal/mol. The DHTSN PES in Ref. [36] has the respective parameters: barrier with height = 3.8 kcal/mol is located at around $(r_{\mathrm{HF}}, r_{\mathrm{HCl}}) = (1.4, 1.3)$ Å; the reaction exothemicity[36,44,45] is −33 kcal/mol. The barrier at position (1.45, 1.30) Å (Table 2) and that at height ≈ 3.5 kcal/mol ∼ 4.0 kcal/mol relative to entrance valley −0.5 kcal/mol are equal to those of the DHTSN PES published in Ref. [36]. But the reaction exothermicity is 8 kcal/mol–10 kcal/mol less. The reasons for this discrepancy may be: a) the peak height of the barrier is quite con-

centrated in a very small region; and entrance valley is quite narrow and steep on the cliff side, so that the relevant values taken optically are rather uncertain. As soon as the resolutions of plot level of r_{HF}, r_{HCl}, and interval (Table 2) are increased to higher than 0.01 Å and 0.01 kcal/mol, respectively, the reaction can be more exothermic, closer to −33 kcal/mol and the barrier height can become closer to 3.8 kcal/mol. b) The number of the original potential energy surface data points are 418, and the resolution of distances r_{HF}, r_{HCl}, and r_{ClF} published is around 0.25 Å (0.5 a_0), which is rougher than 0.05 Å, with which this PES is reproduced and shown in Fig. 2. However, step width within every trajectory along the PES for our calculation is 0.1 fs, which corresponds approximately to 4.5×10^{-4} Å–10^{-3} Å within $E_{rel} = 0.5$ kcal/mol–20 kcal/mol for our title reactions. This distance is far smaller than 0.01 Å mentioned above, which means that the exothermicity of DHTSN PES reproduced should be the same as that of DHTSN published.

Table 2. Parameters of the potential energy contours taken from DHTSN for reactions F + HCl → HF + Cl, H + ClF → HCl + F, and H + ClF → HF + Cl, with the respective bent angels of the transition intermediates. Coordinates are in unit Å, heights, wells, plot level, and interval are in unit kcal/mol.

Reaction	Barrier, entrance, height, position	Barrier, plateau height, position	Well, entrance, depth, position	Well, exit, depth, position	Plot level, min, max, interval
FHCl, 123.5°	≥ 3.0, (1.45, 1.30)	no plateau	−0.5, (3.0, 1.25)	−20, (1.25, ≥ 3.0)	−1, 3, 0.2
HClF, 90°	2.1, (2.0, 1.8)	5.0, (2.95, 3.1)	0.8, (3.05, 1.7)	−50, (1.35, ≥ 3.3)	−1, 5, 0.2
HClF, 120°	2.2, (2.05, 1.75)	5.0, (3.0, 3.2)	−0.5, (3.2, 1.7)	−50, (1.3, ≥ 3.5)	−1, 5, 0.2
HFCl, 90°	2.5, (1.55, 1.65)	no plateau	1.20, (2.8, 1.0)	−20, (0.85, ≥ 3.0)	−1, 5, 0.2
HFCl, 120°	2.6, (1.9, 1.7)	no plateau	1.0, (3.1, 1.0)	−20, (0.8, ≥ 2.5)	−1, 4, 0.2

The fitted PES for reaction H + ClF → HCl + F (Fig. 3, and Table 2) with intermediate [H–Cl–F] at bent angle = 90° has the barrier height 2.1 kcal/mol at (2.0, 1.8) Å, a well with depth 0.8 kcal/mol at (3.05, 1.7) Å in the entrance valley and another well with depth −50 kcal/mol at (1.35, ≥ 3.3) Å in the exit valley, and that at bent angle = 120° has the barrier height 2.2 kcal/mol at (2.05, 1.75) a well with depth −0.5 kcal/mol at (3.2, 1.7) Å in the entrance valley, and another well with depth −50 kcal/mol at (1.3, ≥ 3.5) Å in the exit valley. There are also barriers on the plateau with height 5.0 kcal/mol at (2.95, 3.1) and (3.0, 3.2) Å for bent angles of 90° and 120°, respectively, which however, does not have any influence on the reaction. The plot level for Fig. 3 is min = −1, max = 5, interval = 0.2 kcal/mol, obtained with Origin 8.0 for both angles.

Compared with those mentioned above, the reaction H + ClF → HF + Cl (Fig. 4 and Table 2) with intermediate [H–F–Cl] at bent angle = 90° has the barrier height 2.5 kcal/mol at (1.55, 1.65) Å, well with depth 1.2 kcal/mol at (2.8, 1.0) Å in the entrance valley, and another well with depth −20 kcal/mol at (0.85, ≥ 3.0) Å in the exit valley. The plot level in Fig. 4 is min = −1, max = 5, interval = 0.2, in kcal/mol, obtained with Origin 8.0, and that at bent angle = 120° has the barrier height 2.6 kcal/mol at (1.9, 1.7) Å, a well with depth 1.0 kcal/mol at (3.1, 1.0) Å in the entrance valley and another well with depth −20 kcal/mol at (0.8, ≥ 2.5) Å in the exit valley. There is no extra plateau. The plot level is min = −1, max = 4, interval = 0.2, in kcal/mol, obtained with Origin 8.0.

Regarding the mass values of the atoms involved, the reaction F + HCl → HF + Cl can be classified as H_1+LH_2 →LH_1+H_2, where H_1, H_2, and L represent heavy and light atoms, respectively.[13,17–19] The arabic numbers 1 and 2 are to distinguish two heavy atoms, if they are different. However, the title reactions belong to the type of either L + H_1H_2 →LH_1+H_2, or L + H_1H_2 →LH_2+H_1.[17–19,24]

3.1. Translational enhancement

Locations of the three barriers (Figs. 2–4 and Table 2) of the three reactions mentioned above are "early barriers"[18,19] and they are located in the entrance valley. Generally, the barrier located at the entrance valley (right side of the diagonal) gives rise to translational enhancement definitely, i.e., the value(s) of integral reaction cross section σ of the product (products) is dependent on the relative translational energy E_{rel} of the reactants. Compare with those shown in Fig. 5, integral cross sections of product molecules HCl and HF of the title reactions are directly proportional to the relative translational energy. Regarding to the bent angles of the intermediate geometries of the title reactions, barriers for two reactions at angle = 120° are a little bit higher than those at angle = 90°. They are 2.1 kcal/mol and 2.2 kcal/mol for reaction intermediate [H–Cl–F] in the cases at 90° and 120°, respectively, 2.5 kcal/mol and 2.6 kcal/mol for reaction intermediate [H–F–Cl] (Table 2) in the cases at angles of 90° and 120° respectively. Locations (2.05, 1.75) Å and (1.9, 1.7) Å of barriers for the case of 120° of two title reactions with intermediates [H–Cl–F] and [H–F–Cl], respectively, appear as earlier (closer to the beginning of the entrance valley) barrier (Figs. 3, 4, and Table 2). This means that PESs constructed with bent angle 90° at locations (2.0, 1.8) Å and (1.55, 1.65) Å for the transition intermediates [H–Cl–F] and [H–F–Cl], respectively, imply a small shift from early to not-so-early barrier (closer to the diagonal), accompanied by a similarly precipitous increase in the 2D barrier height (Figs. 3(a) and 4(a)). The reaction on PES with angle 120° should run as an earlier barrier reaction dynamics. The passage around the barrier is narrow for reaction H + ClF→ HF + Cl running from the entrance valley

into the exit valley for both kinds of PESs with bent angles 90° and 120° compared with those of H + ClF → HCl + F. This can be explained as the fact that PES topology of reaction H + ClF → HF + Cl possesses a narrow transit passage around the barrier, resulting in anomalously smaller reaction cross sections[36,44–48] (Fig. 5) compared with those of H + ClF → HCl + F. The narrower transit passage and barrier region at the moment of transformation reaction around the barrier, may be one of the reasons which causes reaction H + ClF → HF + Cl to run "directly" as well as via direct reaction mechanism[46–48] at $E_{\rm rel} \leq 2.5$ kcal/mol, with $b_{\rm max} \leq 2.6$ Å. Direct and migratory manner are mixed for $E_{\rm rel} = 2.5$ kcal/mol–20 kcal/mol (Table 1). The direct manner also makes the p_2(HF) stronger, at $E_{\rm rel} < 2.5$ kcal/mol (Fig. 9 and Table 1). Another reason[46–48] can be that during the reaction of H + ClF → HCl + F, because the mobility of H is greatest to change the nuclear configuration, the mobility of F is the next, that of Cl is smallest; Cl has the largest size and can be assumed to be stationary. During the interaction among H, F, and Cl, H can first be attracted by Cl because of the huge size of Cl yielding HCl. It is also possible that immediately before HCl or even after nascent HCl is produced, H moves around Cl, as soon as H approaches to the F–Cl bond region, H can be more readily attracted by F instead by Cl, because of its larger electronegativity (H = 2.20, F = 3.98, Cl = 3.16). Such a kind of phenomenon is referred to as migratory reaction.[36,46–48] H migration to F appears more possible if $b_{\rm max} \geq 2.6$ Å (Table 1).

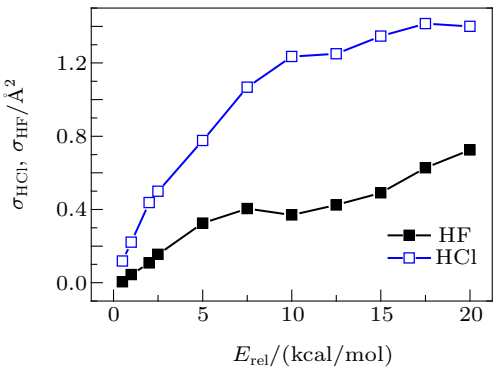


Fig. 5. (color online) Distributions of integral cross sections of product molecules HCl and HF of H + ClF($v = 0, j = 0$) → HCl(v', j') + F, and HF(v', j') + Cl, respectively, at $E_{\rm rel}$ = 0.5 kcal/mol–20 kcal/mol.

The value of σ(HF) is still smaller than that of σ(HCl), though migration helps and increases the production of HF. The width of the entrance channel for the case [H–F–Cl] either at 120° or at 90° is rather narrow compared with the bond length $r_{\rm ClF}$ ($r_{\rm HF} = 0.917$ Å, $r_{\rm HCl} = 1.274$ Å, $r_{\rm ClF} = 1.628$ Å), which may cause the approach of H and ClF as well as the reaction to be difficult. However, the vibrational effect of ClF increases the cross section of HF more effectively than that of [H–Cl–F] (Fig. 6(b)). The width of the entrance channel is a little bit wider for the production of HCl may be one of the reasons why the vibrational enhancement for the production of HCl is rather small. Because the vibrational enhancement of ClF for the production of HF is stronger than that for HCl in the range of $v = 0$–5 (Fig. 6(b)), and the translational enhancement for production of HF keeps increasing, even for $E_{\rm rel} > 20$ kcal/mol (Fig. 5), and a maximum value σ(HCl) = 1.4 Å^2 is asymptotically reached around $E_{\rm rel} = 15$ kcal/mol–20 kcal/mol. The contribution of the migratory effect for the production of HF (Tables 3(a)–3(c)) may be significant so that σ(HF) would be larger than σ(HCl) at a certain higher relative translational energy $E_{\rm rel}$ and a certain higher vibrational energy of ClF. Because the vibrational enhancement of ClF for the production of HF is stronger than that of HCl in the range of $v = 0$–5 (Fig. 6(b)), and the translational enhancement for production of HF keeps increasing, even for $E_{\rm rel} > 20$ kcal/mol (Fig. 5), and a maximum value of σ(HCl) approaches asymptotically $E_{\rm rel} = 17.5$ kcal/mol, contribution of the migratory effect to the production of HF (Tables 3(a)–3(c)) may be significant so that σ(HF) would be larger than σ(HCl) at certain higher relative translational energy $E_{\rm rel}$ and a certain higher vibrational energy of ClF.

There are direct H + ClF →[H–F–Cl]→ HF + Cl, and migration H + ClF →[H–Cl–F]→[H–F–Cl]→ HF + Cl reaction mechanisms for the production of HF molecule whatever is similar to H + ICl → HCl + I,[24] regarding to potential energy contours and reaction mechanisms. This reaction belongs also to the type of L + H_1H_2.

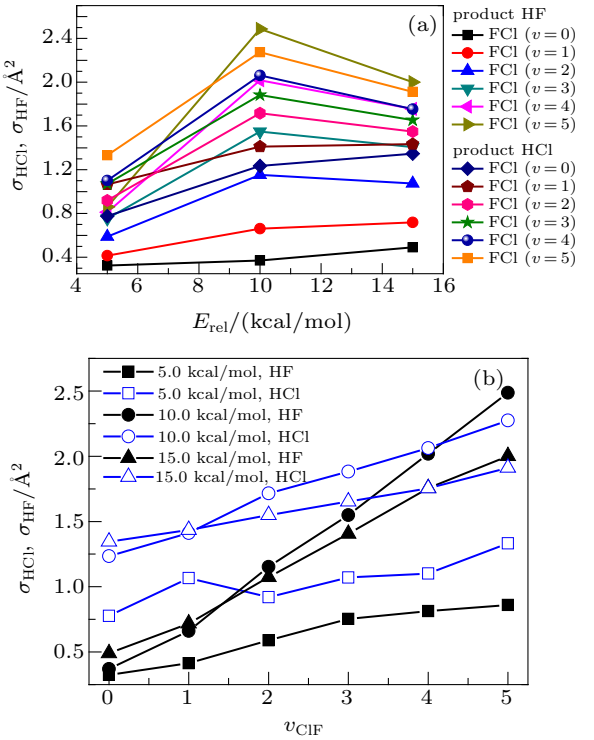


Fig. 6. (color online) Distributions of integral cross sections of HCl and HF, dependent on (a) relative translational energy $E_{\rm rel}$ of the reactants, and (b) vibrational energy states $v = 0$–5 of ClF, of H + ClF ($v = 0$–5, $j = 0$)→ HCl(v', j') + F and HF(v', j') + Cl, respectively, at $E_{\rm rel}$ = 5, 10, and 15 kcal/mol.

Table 3. Distributions of the values of impact parameter b_{max}, number of reactive trajectories n, integral cross sections σ, and alignment $p_2(=\langle \boldsymbol{j}' \cdot \boldsymbol{k} \rangle)$ of product molecules HCl and HF, dependent on the vibrational states v, with 10^4, batches, for reactions H + ClF ($v = 0$–5, $j = 0$) → HCl (v', j') + F and HF (v', j') + Cl, respectively, at relative scatterinag energies (a) 5, (b) 10, and (c) 15 kcal/mol.

Table 3(a)

5/kcal·mol^{-1}		HCl				HF			
v	j	b_{max}/Å	n_{HCl}	σ_{HCl}/Å^2	p_2	b_{max}/Å	n_{HF}	σ_{HF}/Å^2	p_2
0	0	2.855	303	0.7759	−0.2683	2.855	127	0.3252	−0.2207
1	0	3.469	282	1.0661	−0.2175	2.7	181	0.4145	−0.1981
2	0	4	183	0.9199	−0.0927	3.5	153	0.5888	−0.1685
3	0	3.6075	262	1.0712	−0.1003	3.505	195	0.7526	−0.1145
4	0	3.075	371	1.1021	−0.0470	3.21	251	0.8125	−0.0604
5	0	3.35	378	1.3327	−0.0555	3.35	244	0.8603	−0.0964

Table 3(b)

10/kcal·mol^{-1}		HCl				HF			
v	j	b_{max}/Å	n_{HCl}	σ_{HCl}/Å^2	p_2	b_{max}/Å	n_{HF}	σ_{HF}/Å^2	p_2
0	0	2.308	738	1.23503	−0.3453	2.308	221	0.36984	−0.1383
1	0	2.863	548	1.41115	−0.2692	2.59	314	0.66173	−0.0791
2	0	3	607	1.71625	−0.1919	2.875	444	1.15294	−0.0555
3	0	3	666	1.88307	−0.17175	3.15	497	1.54927	−0.0699
4	0	3.5	536	2.06277	−0.1502	3.43	546	2.01804	−0.03485
5	0	3.2	707	2.27441	−0.1731	3.45	665	2.48662	−0.0492

Table 3(c)

15/kcal·mol^{-1}		HCl				HF			
v	j	b_{max}/Å	n_{HCl}	σ_{HCl}/Å^2	p_2	b_{max}/Å	n_{HF}	σ_{HF}/Å^2	p_2
0	0	2.25	828	1.3169	−0.3464	2.4	271	0.4904	−0.1156
1	0	2.25	902	1.4346	−0.2530	2.503	365	0.7184	−0.0436
2	0	2.4875	797	1.5493	−0.2067	2.7	469	1.0741	0.0185
3	0	2.685	730	1.6533	−0.2262	2.8	571	1.4064	−0.0264
4	0	2.8	712	1.7537	−0.2301	2.85	688	1.7556	−0.0443
5	0	3.05	654	1.9113	−0.2430	2.97	722	2.0008	−0.0843

3.2. Vibrational enhancement

The barrier, which is located in the exit valley, i.e., on the left side of the diagonal, is called "late-barrier". The reaction can be more easily achieved through vibrational excitation, so such a molecule is known as a vibrationally enhancing reactant molecule instead of translationally enhancing reactants (with higher relative translational energy of the reactants). The reaction intermediate can smoothly overcome the barrier region, and slip into the exit valley.[17–19] Such a reaction is called vibrationally enhanced reaction. However, both barriers of the title reactions are located in the entrance valleys; there are rather abnormal vibrational enhancements involved (Figs. 6(a), 6(b), and Table 3). The approach of the reactants, either for reaction H + ClF → HCl + F, or H + ClF → HF + Cl, intermediates is formed as either [H–Cl–F] or [H–F–Cl] around the barrier regions. In this 3-atom interacting region, H and Cl can establish rather higher vibrational and rotational motions, despite a long distance between H and Cl.[24,36,40,41,44–48] In other words, H–Cl molecule can tolerate long distance stretching and higher vibrational states than H–F molecule. This means that nascent HCl molecule can also be yielded in spite of the rather far distance between H and Cl, more easily than HF molecule, as the H–Cl is likely to rotate and vibrate rapidly, and their durations are short compared with the dissociation time of the intermediate. At this moment, the H atom keeps running around, and provokes vibrational and rotational motions between H and F too. It is plausible that H could be attracted by either the F or Cl atom to form the product molecule HF or HCl. Because the attraction between H and F is stronger than that between H and Cl, HF should be more easily produced. However, the barrier with 2.6 kcal/mol and at bent angle 120° to form HF (Table 2) is slightly higher, or more difficult than that with 2.2 kcal/mol and at the same bent angle to form HCl (Table 2); and the transformation passage around the barrier region (Figs. 3 and 4) for the formation into HF is rather narrow compared with that for formation into HCl. Additionally, the steeper entrance valley for approach of H to F and barrier region of either [H–F–Cl] or [H–Cl–F] may cause the production of HF to be rather difficult compared with the production of HCl (Figs. 3 and 4).

3.3. Rotational energy specific translational enhancement

Referring to Fig. 7 and Tables 4(a)–4(h), there are slight translational enhancements for the reactant molecule ClF with

internal energy states ($v = 0$, $j = 3, 6, 9$), i.e., rotational energy-dependent translational enhancements, or rotational energy specific translational enhancement for both title reactions at $E_{rel} = 5$, 10, and 15 kcal/mol. All reactive cross sections of product molecules HCl with $j = 0$, 3, 6, and 9 of ClF at all three relative translational energies $E_{rel} = 5$, 10, and 15 kcal/mol are larger than those of HF with the respective rotational energy states of reactant molecule ClF (Fig. 7 and Tables 4(a)–4(h)). The rotational energy j dependence of the translational enhancement of each title reaction is only minimally differentiable. In other words, according to our results given in Fig. 7 the translational energy enhancement with specific rotational energy state j of the reactant molecule ClF of each of the title reaction is still unclear.

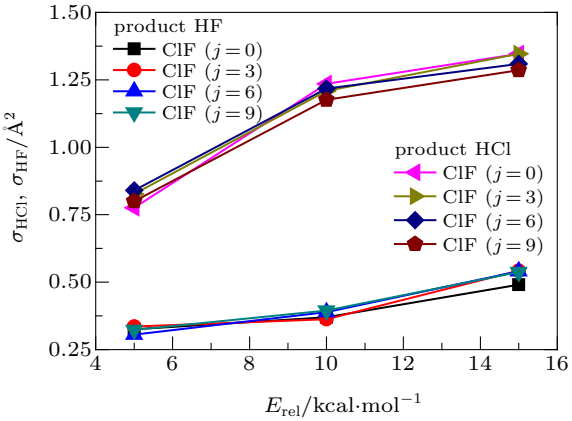


Fig. 7. (color online) Distributions of integral cross sections of HCl and HF of $H + ClF(v = 0, j = 0, 3, 6, 9) \rightarrow HCl(v', j') + F$ and $HF(v', j') + Cl$, respectively, at $E_{rel} = 5$, 10, and 15 kcal/mol, dependent on the rotational angular momenta j of the reactant molecule ClF.

Table 4. Distributions of the values of impact parameter b_{max}, number of reactive trajectories n, integral cross section σ, and alignment $p_2(= \langle \boldsymbol{j}' \cdot \boldsymbol{k} \rangle)$ of HCl and HF, dependent on the rotational states j, with 10000 batches, for reactions $H + ClF(v = 0, j = 0, 3, 6, 9) \rightarrow HCl(v', j') + F$ and $HF(v', j') + Cl$, at relative scattering energies (a) 0.5, (b) 1, (c) 2, (d) 5, (e) 10, (f) 12.5, (g) 15, (h) 20 kcal/mol.

Table 4(a)

0.5/kcal·mol^{-1}		HCl				HF			
v	j	b_{max}/Å	n_{HCl}	σ_{HCl}/Å^2	p_2(HCl)	b_{max}/Å	n_{HF}	σ_{HF}/Å^2	p_2(HF)
0	0	2.55	58	0.11848	−0.27645	1.5	7	0.00495	−0.4216
0	3	2.525	49	0.09815	−0.30775	0.9	10	0.00254	−0.1732
0	6	2.45	56	0.1056	−0.17042	0.9	15	0.00382	−0.24629
0	9	2.525	41	0.08212	−0.19956	1.75	10	0.00962	−0.26111

Table 4(b)

1/kcal·mol^{-1}		HCl				HF			
v	j	b_{max}/Å	n_{HCl}	σ_{HCl}/Å^2	p_2(HCl)	b_{max}/Å	n_{HF}	σ_{HF}/Å^2	p_2(HF)
0	0	2.5625	107	0.22073	−0.26089	1.9	39	0.044230	−0.38500
0	3	2.6	109	0.23149	−0.21036	1.5	37	0.026154	−0.32591
0	6	2.6615	110	0.24479	−0.16489	2	30	0.037699	−0.33375
0	9	2.67	86	0.19261	−0.19443	2.3	23	0.038224	−0.18130

Table 4(c)

2/kcal·mol^{-1}		HCl				HF			
v	j	b_{max}/Å	n_{HCl}	σ_{HCl}/Å^2	p_2(HCl)	b_{max}/Å	n_{HF}	σ_{HF}/Å^2	p_2(HF)
0	0	2.75	184	0.43715	−0.2792	2	86	0.1081	−0.3008
0	3	2.75	155	0.36825	−0.2665	2.7	52	0.1191	−0.2912
0	6	2.7375	181	0.4261	−0.1678	2.7	48	0.1099	−0.2341
0	9	2.7	191	0.4374	−0.1587	1.92	85	0.0984	−0.0945

Table 4(d)

5/kcal·mol^{-1}		HCl				HF			
v	j	b_{max}/Å	n_{HCl}	σ_{HCl}/Å^2	p_2(HCl)	b_{max}/Å	n_{HF}	σ_{HF}/Å^2	p_2(HF)
0	0	2.855	303	0.7759	−0.2683	2.855	127	0.3252	−0.2207
0	3	2.855	323	0.8271	−0.2399	2.855	131	0.33545	−0.2024
0	6	3.29	247	0.8399	−0.2309	2.91	115	0.3059	−0.1968
0	9	2.88	307	0.8000	−0.2218	2.88	124	0.3231	−0.1751

Table 4(e)

10/kcal·mol^{-1}		HCl				HF			
v	j	b_{max}/Å	n_{HCl}	σ_{HCl}/Å^2	p_2(HCl)	b_{max}/Å	n_{HF}	σ_{HF}/Å^2	p_2(HF)
0	0	2.308	738	1.2350	−0.35475	2.308	221	0.3698	−0.1383
0	3	2.35	697	1.2093	−0.3389	2.23	232	0.36245	−0.1845
0	6	2.36	696	1.2178	−0.33425	2.35	224	0.3886	−0.1609
0	9	2.35	678	1.1763	−0.3406	2.358	226	0.3948	−0.1244

Table 4(f)

12.5/kcal·mol^{-1}		HCl				HF			
v	j	b_{max}/Å	n_{HCl}	σ_{HCl}/Å^2	p_2(HCl)	b_{max}/Å	n_{HF}	σ_{HF}/Å^2	p_2(HF)
0	0	2.2925	757	1.2499	−0.3590	2.2325	271	0.4243	−0.0896
0	3	2.2875	800	1.3151	−0.3628	2.25	262	0.4167	−0.0956
0	6	2.275	795	1.29265	−0.3585	2.225	283	0.44015	−0.1410
0	9	2.25	800	1.27235	−0.3656	2.3	263	0.4371	−0.1133

Table 4(g)

15/kcal·mol^{-1}		HCl				HF			
v	j	b_{max}/Å	n_{HCl}	σ_{HCl}/Å^2	p_2(HCl)	b_{max}/Å	n_{HF}	σ_{HF}/Å^2	p_2(HF)
0	0	2.25	828	1.3169	−0.3464	2.4	271	0.4904	−0.1156
0	3	2.24	848	1.3367	−0.3440	2.25	341	0.5423	−0.0487
0	6	2.20	861	1.3092	−0.3450	2.22	349	0.5404	−0.0728
0	9	2.2505	808	1.2856	−0.3514	2.22	347	0.5373	−0.0987

Table 4(h)

20/kcal·mol^{-1}		HCl				HF			
v	j	b_{max}/Å	n_{HCl}	σ_{HCl}/Å^2	p_2(HCl)	b_{max}/Å	n_{HF}	σ_{HF}/Å^2	p_2(HF)
0	0	2.21	912	1.3994	−0.2906	2.24	460	0.7251	−0.01755
0	3	2.23	894	1.3967	−0.2952	2.25	476	0.75705	−0.02343
0	6	2.24	894	1.4092	−0.2996	2.26	463	0.7429	−0.023595
0	9	2.24	889	1.40135	−0.30015	2.3	432	0.7179	−0.02469

3.4. Rotational enhancement

There are no rotational enhancements with $j = 3$, 6, and 9 rotationally prepared ClF obtained in our results (Figs. 8(a), 8(b) and Tables 4(a)–4(h)). According to the above pictorial explanation of the three-atom interaction with not only vibrational but also translational enhancements involved during the title reactions, the rotational enhancement should be investigated with higher, even much higher rotationally prepared reactant molecule ClF. It is possible that the rotational enhancement, even with very high $j \geq 30$–50 for reaction H + ClF → HF + Cl is rather weak because of its narrow and steep passage of the entrance valley and barrier region compared with those for the reaction H + ClF → HCl + F.

3.5. Alignment

It is understandable that the alignment of the product molecule HF is rather weak, even decreasing in proportion to the relative translational energy E_{rel}, compared with that of HCl (Fig. 9 and Table 2). Under the situation of slow approach of H and ClF around the translational energy threshold $E_{rel} \leq 0.2$ kcal/mol, HF molecule shows stronger alignment than HCl because of the strong and abrupt attraction between H and F compared with that between H and Cl. The steep and narrow transit passage may be also one of the reasons. Regarding a highly vibrationally excited product molecule, either HCl or HF, the higher vibrationally excited product molecule are more weakly aligned as shown in Fig. 10 and given in Tables 3(a)–3(c). In general, HF (v = 0–5, $j = 0$) are more weakly aligned than HCl (v = 0–5, $j = 0$), respectively, at E_{rel} = 5, 10, and 15 kcal/mol. At higher relative translational energy E_{rel} (among 5, 10, and 15 kcal/mol), product molecules HCl are more strongly aligned than HF for each vibrational energy state of v = 0–5 of reactant molecule ClF. On the contrary, it

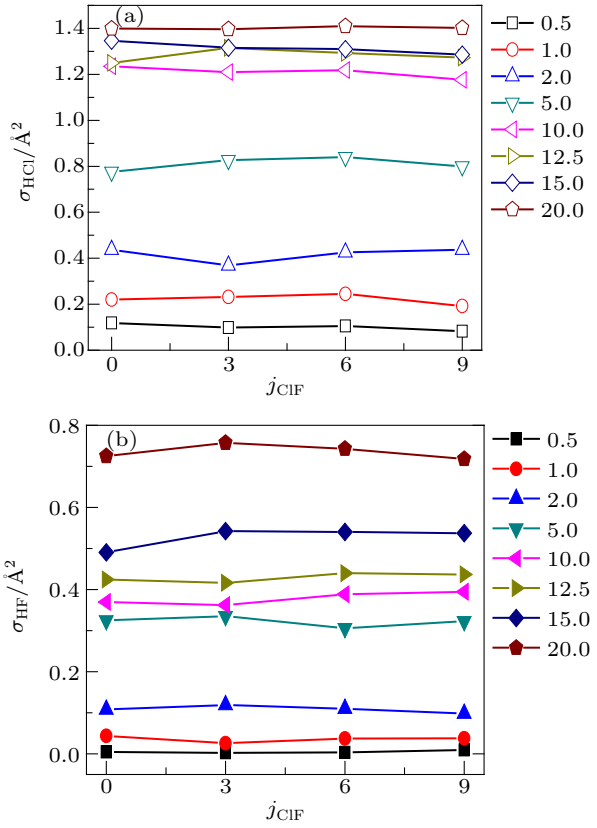


Fig. 8. (color online) Distributions of integral cross sections of (a) HCl of H + ClF($v = 0, j = 0,3,6,9$) → HCl(v', j') + F, and (b) HF of H + ClF($v = 0, j = 0,3,6,9$) → HF(v', j') + Cl, respectively, at E_{rel} = 0.5 kcal/mol–20 kcal/mol, dependent on the rotational angular momenta j of the reactant molecules ClF.

is not the case for HF. HF molecules with $v = 0$, and $j = 0$ of ClF, should be more highly aligned than HCl with the same zero internal energies of ClF, at lower E_{rel} (Fig. 9) around the translational threshold. How the influences of height and steepness of the barrier, width, and steepness of the entrance valley on the alignment of the product molecule are dependent on the vibrational states $v = 0$–5 of the reactant molecule ClF must be further investigated. The alignments of HCl are directly proportional to E_{rel} of the reactant and vibrational states of the reactant molecule ClF. The reason that is or is not for the alignments of HF with translationally and vibrationally enhancing reactants H and ClF, and reactant molecule ClF should be also interesting for the further investigation. Whether, when and under which conditions the extra plateau on the PES of H + ClF → HCl + F may influence the reaction dynamics, can be significant for the further investigation too.

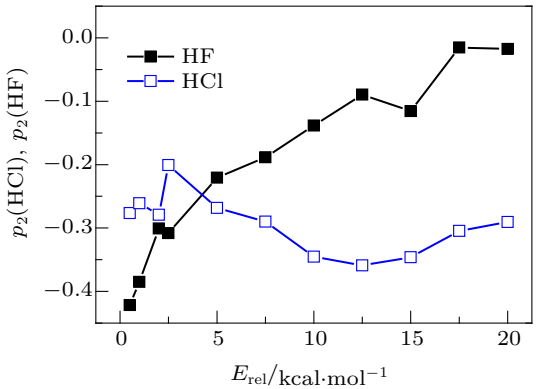


Fig. 9. (color online) Distributions of alignments of product molecules HCl and HF of H + ClF ($v = 0, j = 0$) → HCl (v', j') + F and HF (v', j') + Cl, respectively, at E_{rel} = 0.5 kcal/mol–15 kcal/mol.

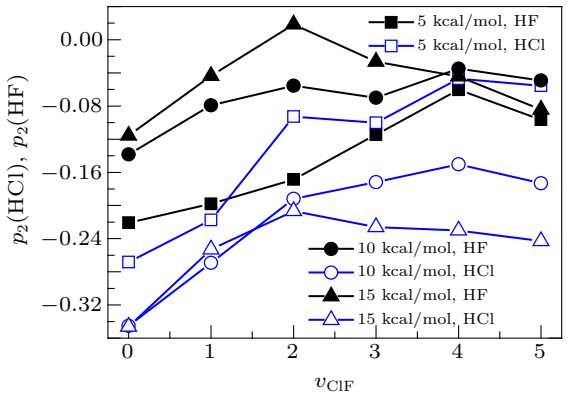


Fig. 10. (color online) Distributions of alignments of HCl and HF, dependent on the vibrational states $v = 0$–5 of ClF of H + ClF ($v = 0$–5, $j = 0$) → HCl (v', j') + F and HF (v', j') + Cl, respectively, at E_{rel} = 5, 10, and 15 kcal/mol.

4. Conclusions

The three-atomic interaction systems of e.g., H, Cl, and F, with intermediate written as either [HClF], [ClHF] or [HFCl] can be reached from either of the reactions H + ClF, Cl + HF, and F + HCl. There is no difference among three kinds of the written forms [HClF], [ClHF], and [HFCl]. Ground potential energy surface[36] (Fig. 2) for reaction F(^{2}P) + HCl → HF + Cl(^{2}P) is therefore applicable for our title reactions H + ClF ($v = 0$–5, $j = 0, 3, 6, 9$) → HCl + F and H + ClF ($v = 0$–5, $j = 0, 3, 6, 9$) → HF + Cl, at E_{rel} = 0.5 kcal/mol–20 kcal/mol. The obtained DHTSN PES of Deskevich *et al.*[36] is first tested and inserted into the program Symplectic for trajectory calculation. The dependences of integral cross sections of the product molecules HCl and HF with ground internal energies ($v = 0$, $j = 0$) on the translational energies at E_{rel} = 0.5 kcal/mol–20 kcal/mol, the dependences of integral cross sections on the internal energy state of the reactant molecule with ClF ($v = 0$–5, $j = 0$) at E_{rel} = 5, 10, 15 kcal/mol, and ClF ($v = 0$, $j = 0, 3, 6, 9$) at E_{rel} = 0.5 kcal/mol–20 kcal/mol, are obtained. The respective translational (Figs. 5, 6(a), and Table 1), vibrational (Figs. 6(a), 6(b), and Table 3), rotational energy specific translational (Fig. 7 and Tables 4(a)–4(h)), and rotational (Figs. 8(a), 8(b), and Tables 4(a)–4(h)) enhancements of the title reactions are found and investigated. The influences of the potential energy contours (Figs. 3 and 4), as well as heights and positions of the barriers and valleys (Table 2) of the respective title reactions, on the reaction mechanisms are investigated and discussed. Further investigations on much higher rotationally excited reactant molecules with j higher than 30, even 50 are necessary, so that how and how far the rotational energies of the reactant molecule either HCl or HF will influence or be mixed into the translational energy enhancement of the title reactions should be further studied.

PESs of three involved reactions are very different, though there is only one intermediate of three atoms. Both title reactions are early barrier reactions,[17–19,23,24] where barrier of reaction H + ClF → HCl + F (Figs. 3(a), 3(b), and Table 2) is earlier than that of H + ClF → HF + Cl (Figs. 4(a), 4(b), and Table 2). The two PESs of the title reactions with the respective bent intermediate at angle 90° and 120° are plotted and compared. The height of the reaction barrier of H + ClF → HCl + F is approximately 5 kcal/mol lower, r_{HCl} and r_{ClF} of that are larger than those of H + ClF → HF + Cl, for both cases of bent intermediates at 90° and 120°. Location of the barrier of reaction of H + ClF → HCl + F is far from the "cliff" of the entrance and exit valleys compared with that of H + ClF → HF + Cl. The larger bent angle (120°) of the reaction intermediate of either of H + ClF → HCl + F or H + ClF → HF + Cl is associated with slightly higher reaction barrier, larger r_{HCl} and r_{HF}, and smaller r_{ClF}, respectively (Figs. 3, 4, and Table 2). In other words, the contours of the entrance valleys are slightly squeezed and precipitous; the region of the reaction barrier is a little bit wider or looser. Any of the translational, vibrational, and rotational motions of either reactant ClF or product molecule HF in the reaction H + ClF → HF + Cl should be more difficult because of the narrow entrance valley and small barrier region, than those in

$H + ClF \rightarrow HCl + F$. Although the smaller width of the entrance channel and size of the barrier region of the reaction $H + ClF \rightarrow HF + Cl$ at $E_{rel} = 0.5$ kcal/mol–20 kcal/mol cause the smaller integral cross sections (Fig. 5), the reaction is vibrationally enhanced rather effectively compared with those of $H + ClF \rightarrow HCl + F$ at $E_{rel} = 0.5$ kcal/mol–20 kcal/mol (Figs. 6(a) and 6(b)). The optimal angles of the bent intermediates during the transformation at barriers of the title reactions should be found, so that the dynamics closer to real reactions can be established.

The translational enhancements due to the values of relative translational energy E_{rel} of the reactants of the title reactions are evident. Surprisingly, the vibrational enhancements are also due to the vibrational energy states of the reactant molecules. The broader entrance valley and barrier region of $H + ClF \rightarrow HCl + F$ allow the higher reactivity, easier formation of long bond length stretching mode, i.e., larger reactive cross sections of HCl. During the interaction among the three atoms, the wandering H atom can be attracted by F instead of Cl, or go from Cl to F, because of the larger electronegativity of F; as soon as H comes closer to F, the so-called migration of F then happens. The entrance valley and barrier region are relatively narrow and steep; H atom comes mostly closer to F as well as with smaller impact parameter, during the reaction $H + ClF \rightarrow HF + Cl$ at $E_{rel} \leq 2.5$ kcal/mol (Table 1). This is the so called direct reaction. Product HF can be obtained via two kinds of reaction mechanisms,[24,36,46–48,78] i.e., migratory reaction and direct reaction, during the reaction of $H + ClF$. How far the migratory effect by which the values of E_{rel} (Fig. 5) and v(ClF) (Fig. 6(b)) are larger will keep increasing the reaction cross section σ(HF) of the reaction $H + ClF \rightarrow HF + Cl$, even larger than σ(HCl) of the reaction $H + ClF \rightarrow HCl + F$ must still be investigated. The extra plateau in the reaction of $H + ClF \rightarrow HCl + F$ should not have any significant influence on the reactions under the given conditions.

Acknowledgment

As an associate professor of the Department of Chemical and Materials Engineering of the National Kaohsiung University of Applied Sciences (KUAS), Kaohsiung, Taiwan, and on leave from Victor Basic Research Laboratory e. V. (VBR), Bielefeld, Germany, Chao wishes to thank Prof. K. L. Han of the Dalian Institute of Chemical Physics of the Chinese Academy of Sciences for providing the QCT-PDDCS code, very helpful discussion, and hospitalities. Chao is also indebted to the State Key Laboratory of Molecular Reaction Dynamics of the Dalian Institute of Chemical Physics of the Chinese Academy of Sciences, and VBR in Bielefeld, Germany for the financial support.

References

[1] London F 1928 *Sommerfeld Festschrift* (Leipzig: S. Hirzel) p. 104
[2] London F 1929 *Z. Elektrochem.* **35** 552
[3] Heitler W and London F 1927 *Z. Physik* **44** 455
[4] Eyring H and Polanyi M 1931 *Z. Phys. Chem. Abt. B* **12** 279
[5] Sato S 1955 *J. Chem. Phys.* **23** 592
[6] Sato S 1955 *J. Chem. Phys.* **23** 2465
[7] Sato S 1955 *Bull. Chem. Soc. Jpn.* **28** 450
[8] Wall F T, Hiller L A Jr and Mazur J 1958 *J. Chem. Phys.* **29** 255
[9] Wall F T, Hiller L A Jr and Mazur J 1961 *J. Chem. Phys.* **35** 1284
[10] Program No. QCPE273, version of 1961 of the Quantum Chemistry Program Exchange (QCPE), University of Indiana, Bloomingtom, USA
[11] Wu V W K 1996 *Verhandl. DPG.* **60** 626 MO2.21
[12] Blais N C and Bunker D L 1962 *J. Chem. Phys.* **37** 2713
[13] Blais N C and Bunker D L 1963 *J. Chem. Phys.* **39** 315
[14] Bunker D L and Blais N C 1964 *J. Chem. Phys.* **41** 2377
[15] Karplus M and Raff L M 1964 *J. Chem. Phys.* **41** 1267
[16] Polanyi J C and Rosner S D 1963 *J. Chem. Phys.* **38** 1028
[17] Kuntz P J, Nemeth E M, Planyi J C, Rosner S D and Young C E 1966 *J. Chem. Phys.* **44** 1168
[18] Polanyi J C and Wong W H 1969 *J. Chem. Phys.* **51** 1439
[19] Hodgson B A and Polanyi J C 1971 *J. Chem. Phys.* **55** 4745
[20] Polanyi J C 1972 *Accounts Chem. Res.* **5** 161
[21] Kirsch L J and Polanyi J C 1972 *J. Chem. Phys.* **57** 4498
[22] Ding A M G, Kirsch L J, Perry D S and Polanyi J C 1973 *Faraday Disc. Chem. Soc.* **55** 252
[23] Brandt D and Polanyi J C 1978 *Chem. Phys.* **35** 23
[24] Polanyi J C, Schreiber J L and Skrlac W J 1979 *Faraday Disc. Chem. Soc.* **67** 66
[25] Han K L, He G Z and Lou N Q 1993 *Chin. Chem. Lett.* **4** 517
[26] Han K L, He G Z and Lou N Q 1996 *J. Chem. Phys.* **105** 8699
[27] Wang M L, Han K L and He G Z 1998 *J. Chem. Phys.* **109** 5446
[28] Wang M L, Han K L and He G Z 1998 *J. Phys. Chem. A* **102** 10204
[29] Chen, M D, Han K L and Lou N Q 2003 *J. Chem. Phys.* **118** 4463
[30] Aquilanti V, Pirani F, Cappelletti D, Vecchiocattivi F and Kasai T 2004 *Theory of Chemical Reaction Dynamics* (Netherland: Springer) Vol. **145**, pp. 243–251
[31] Han K L and Sun B F 2009 *Potential Energy Surface and Molecular Scattering Theory*, (Changchun: Jilin University Press) p. 267 (ISBN 978-7-5601-4080-3)
[32] Wang M L, Han K L, Zhan J P, Wu V W K, He G Z and Lou N Q 1997 *Chem. Phys. Lett.* **278** 307
[33] Sayós R, Hernando J and Hijazo J 1999 *Phys. Chem. Chem. Phys.* **1** 947
[34] Sayós, R, Hernando R J, Francia R and González M 1999 *Phys. Chem. Chem. Phys.* **2** 523
[35] Hayes M Y, Deskevich M P, Nesbitt D J, Takahashi K and Skodje R T 2006 *J. Phys. Chem. A* **110** 436
[36] Deskevich M P, Hayes M Y, Takahashi K, Skodje R T and Nesbitt D J 2006 *J. Chem. Phys.* **124** 224303
[37] Zolot A M and Nesbitt D J 2007 *J. Chem. Phys.* **127** 114319
[38] Yin S H, Guo M X, Li L, Li X P and Zhang Y H 2010 *Chin. Sci. Bull.* **57** 3868
[39] Feng P and Chu T S 2011 *J. Comput. Sci. Eng.* **1** 18
[40] Würzberg E and Houston P L 1980 *J. Chem. Phys.* **72** 5915
[41] Beadle P, Dunn M R, Jonathan N B H, Liddy J P and Naylor J C 1978 *J. Chem. Soc., Faraday Trans. II* **74** 2170
[42] Kornweitz H and Persky A 2004 *J. Phys. Chem. A* **108** 140
[43] Fishchuk A V, Wormer P E S and van der Avoird A 2006 *J. Phys. Chem. A* **110** 5273
[44] Tamagake K and Setser D W 1979 *J. Phys. Chem.* **83** 1000
[45] Sung J P, Malins R J and Setser D W 1979 *J. Phys. Chem.* **83** 1007
[46] Chen L, Pan Y M, Cai Z S and Zhao X Z 1998 *Sci. China Ser. B* **41** 97
[47] Du F P, Chen L, Cai Z S, Pan Y M and Zhao X Z 1999 *Acta Phys. Chim. Sin.* **15** 593
[48] Eades R A and Dunning T H Jr 2008 *J. Chem. Phys.* **75** 2008
[49] Wu V W K 2011 *Phys. Chem. Chem. Phys.* **13** 9407
[50] Chao(Wu) V W K 2012 Additions & Corrections, *Phys. Chem. Chem. Phys.* **14** 16784
[51] Yin S H, Guo M X, Zou J H, Xu X S, Che L, Li L and Gao H 2012 *J. Theor. Comput. Chem.* **11** 791
[52] Yue X F and Miao X Y 2011 *J. Chem. Sci.* **123** 21

[53] Merritt J M, Küpper J and Miller R E 2005 *Phys. Chem. Chem. Phys.* **7** 67
[54] Zolot A M and Nesbitt D J 2007 *J. Chem. Phys.* **127** 114319
[55] Tang B Y, Yang B H, Han K L, Zhang R Q and Zhang J Z H 2000 *J. Chem. Phys.* **113** 10105
[56] Quéméner G and Balakrishnan N 2008 *J. Chem. Phys.* **128** 224304
[57] Schatz G C 2000 *Science* **288** 1599
[58] Alexander M H, Manolopoulos D E and Werner H J 2000 *J. Chem. Phys.* **113** 11084
[59] Xie T X, Zhang Y, Zhao M Y and Han K L 2003 *Phys. Chem. Chem. Phys.* **5** 2034
[60] Chu T S, Zhang Y and Han K L 2006 *Int. Rev. Phys. Chem.* **25** 201
[61] Berry M J and Pimentel G C 1969 *J. Chem. Phys.* **51** 2274
[62] Wu V W K 2010 *Chin. J. Chem. Phys.* **23** 149
[63] Wu V W K, Chung M Y and Kure(Ko) F 2010 *J. Mol. Struct.* **983** 1
[64] Chao(Wu) V W K 2013 *J. Theor. Comput. Chem.* **12** 1250104
[65] Chao(Wu) V W K in preparation
[66] Wei Q and Wu V W K 2009 *Mol. Phys.* **107** 1453
[67] Wei Q, Wu V W K and Zhou B 2009 *J. Theor. Comput. Chem.* **8** 1177
[68] Wei Q, Li T, Zhou B and Wu V W K 2009 *J. Mol. Struct. Theochem.* **913** 162
[69] Xiao J, Wang M S and Yang C L 2011 *Chin. Phys. Lett.* **28** 013101
[70] Yue X F and Wang T 2011 *Chin. Phys. Lett.* **28** 023101
[71] Zhao L, Liu C Z and Sun P 2011 *Chin. Phys. Lett.* **28** 083101
[72] Shi D H, Sun J F and He X H 2011 *Chin. Phys. B* **20** 078201
[73] Xu Z H and Zong F J 2011 *Chin. Phys. B* **20** 063104
[74] Xiao J, Yang C L and Wang M S 2012 *Chin. Phys. B* **21** 043101
[75] Yang T G, Yuan J C, Cheng D H and Chen M D 2013 *Commun. Comput. Chem.* **1** 15
[76] Kuo Y H, Zhang F Y and Ma H Z 2013 *Commun. Comput. Chem.* **1** 99
[77] Wu W K, Reaktive Streuung zwischen Kalium, Barium und den Wasserstoffhalogeniden HCl und HBr, Dr.rer.nat. Dissertation, Faculty of Physics, University of Bielefeld, Bielefeld, Germany, January 23, 1986, 268 pages
[78] Wu V W K, Han K L and He G Z 1997 *Chem. Lett.* **309** 841
[79] Han K L, Zheng X G, Sun B F, He G Z and Zhang R Q 1991 *Chem. Phys. Lett.* **181** 474
[80] Han K L, He G Z and Lou N Q 1991 *Chem. Phys. Lett.* **178** 528